NRL Memorandum Report 5236

On the Convective Properties of the Resistive Hose Instability in an Intense Relativistic Electron Beam

Y. Y. LAU AND M. LAMPE

Plasma Theory Branch
Plasma Physics Division

December 30, 1983

This research was supported by the Defense Advanced Research Projects Agency under ARPA Order 4395, Amendment No. 9.

NAVAL RESEARCH LABORATORY
Washington, D.C.

SECURITY CLASSIFICATION OF THIS PAGE (When Data Entered)

REPORT DOCUMENTATION PAGE

READ INSTRUCTIONS BEFORE COMPLETING FORM

1. REPORT NUMBER: NRL Memorandum Report 5236
2. GOVT ACCESSION NO.: AD-A137 527
3. RECIPIENT'S CATALOG NUMBER:

4. TITLE (and Subtitle): ON THE CONVECTIVE PROPERTIES OF THE RESISTIVE HOSE INSTABILITY IN AN INTENSE RELATIVISTIC ELECTRON BEAM

5. TYPE OF REPORT & PERIOD COVERED: Interim report on a continuing NRL problem.

6. PERFORMING ORG. REPORT NUMBER:

7. AUTHOR(s): Y.Y. Lau and M. Lampe

8. CONTRACT OR GRANT NUMBER(s):

9. PERFORMING ORGANIZATION NAME AND ADDRESS: Naval Research Laboratory, Washington, DC 20375

10. PROGRAM ELEMENT, PROJECT, TASK AREA & WORK UNIT NUMBERS: 47-0900-0-3

11. CONTROLLING OFFICE NAME AND ADDRESS: Defense Advanced Research Projects Agency, Arlington, VA 22209

12. REPORT DATE: December 30, 1983

13. NUMBER OF PAGES: 30

14. MONITORING AGENCY NAME & ADDRESS (if different from Controlling Office): Naval Surface Weapons Center, Silver Spring, MD 20910

15. SECURITY CLASS. (of this report): UNCLASSIFIED

15a. DECLASSIFICATION/DOWNGRADING SCHEDULE:

16. DISTRIBUTION STATEMENT (of this Report)

Approved for public release; distribution unlimited.

17. DISTRIBUTION STATEMENT (of the abstract entered in Block 20, if different from Report)

18. SUPPLEMENTARY NOTES

This research was supported by the Defense Advanced Research Projects Agency under ARPA Order 4395, Amendment No. 9.

19. KEY WORDS (Continue on reverse side if necessary and identify by block number)

Charged particle beam
Electron beam
Intense relativistic electron beam
Beam propagation
Hose instability
Resistive instabilities

20. ABSTRACT (Continue on reverse side if necessary and identify by block number)

We examine the convective characteristics of the resistive hose instability of a charged particle beam propagating in weakly ionized gas. We use a model which includes a plasma return current and a constant rate of plasma electrical conductivity production by the beam. When the spread mass model is adopted, the hose instability is shown, in all cases, to be convective in the beam frame, with the amplifying

(Continues)

DD FORM 1 JAN 73 1473 EDITION OF 1 NOV 65 IS OBSOLETE
S/N 0102-014-6601

SECURITY CLASSIFICATION OF THIS PAGE (When Data Entered)

20. ABSTRACT (Continued)

disturbances propagating from the beam head toward the beam tail, regardless of the amount of return current. The minimum speed of propagation for the amplifying disturbance is typically 1/3 to 1/2 of the group velocity associated with the maximum aplification rate. The implications of this result are explored.

CONTENTS

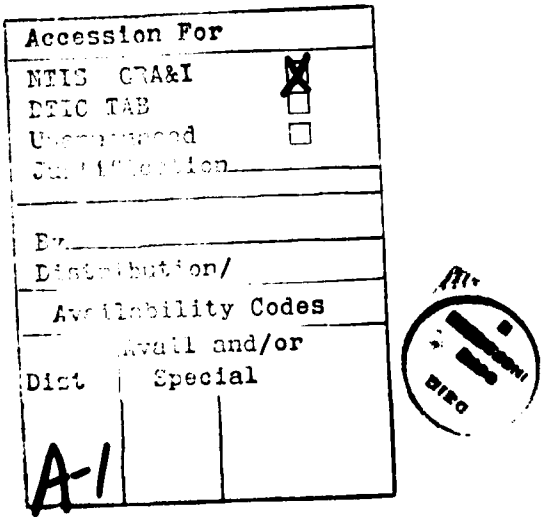

ON THE CONVECTIVE PROPERTIES OF THE RESISTIVE HOSE INSTABILITY IN AN INTENSE RELATIVISTIC ELECTRON BEAM

I. Introduction

The resistive hose instability is a dominant instability of an intense relativistic electron beam propagating in a weakly ionized or initially unionized gas. It has been subject to a variety of experimental[1,2] and theoretical[3-8] studies in recent years. Although the formulation of the physics involved in beam propagation is a difficult problem, even as regards the construction of an equilibrium, remarkable progress has been made in understanding the hose instability by means of highly simplified models. At present, there is substantial qualitative correlation among simple analytic theory, experiment, particle simulation, and other techniques of numerical analysis.

There are certain minimum requirements that must be satisfied by any acceptable model of the hose instability. For example, the early work based on the "rigid beam model"[9] or on the assumption of a constant betatron[10] frequency for all beam electrons indicated that the instability is absolute in the frame co-moving with the beam. More realistic models, such as the spread mass model,[3] or the multicomponent model,[4] indicate that the instability is of a convective nature. However, direct examination of the dispersion relation does not yield much information on the minimum velocity of convection of the amplifying waves, which may be important if one wants to assess the effect of the beam head erosion on the evolution of the instability. Furthermore, recent work[4,5,8] has emphasized that a plasma return current destabilizes the hose instability, and even leads to nonvanishing spatial amplification rates at very low frequency, thereby leading to the speculation that the hose instability may indeed become absolute for sufficiently large return current fraction.

Manuscript approved October 11, 1983.

In the present paper, we study the space-time evolution of the resistive hose instability. We include the effects of plasma return current as well as a self-consistent treatment of the plasma electrical conductivity increase along the beam axis, due (for example) to additional beam-collisional ionization of the gas. The analysis is essentially one-dimensional (axial) in space, and is thus restricted mainly to the beam body,[8] the region behind the pinch point[11,12] where the beam current and radius may be assumed to be roughly constant, and dependence on radial position is easily separated out. Under the simplifying assumptions enumerated at the beginning of Section II, we show that the resistive hose instability is always convective, regardless of the level of the return current. This conclusion results from our examination of the Green's function[13] constructed from the dispersion relation which was derived by Lampe, Sharp, and Hubbard[8] for the spread mass model. In Section III, we extend our analysis to calculate in more detail the evolution of amplifying disturbances based on an ad hoc simplification of the dispersion relation. We find that there is a minimum speed of propagation for amplifying waves. This minimum speed is model dependent, but is typically at most half of the speed associated with the maximum convective growth. This last statement holds throughout the vast parameter space surveyed. The maximum spatial amplification rate is just the value expected from the dispersion relationship.

II. The Model

In this section, we describe our model of the relativistic electron beam. We show here that the resistive hose instability is always convective, when the spread mass model is adopted. We postpone to the next section a calculation of the propagation characteristics.

Our analysis applies to the main body of the beam, at a distance sufficiently far from the beam head. The following simplifying assumptions are introduced: (a) The electron beam is highly relativistic and paraxial, with long betatron wavelength compared with the beam radius.[3-5] (b) The electrical conductivity of the plasma channel is high enough that the charge relaxation length is short compared with beam radius.[3-9] (c) The beam current density $J_{bo}(r)$, plasma current density $J_{po}(r)$, and the conductivity $\sigma_o(r)$, all assume the same Bennett profile and are constant or slowly varying in z and t.[8] (d) The plasma return current I_p is a constant fraction f of the beeam current I_b, with the convention that f is negative when the plasma current flows in the opposite direction to the beam current.[4,5,8] (e) The rate of increase of the equilibrium electrical conductivity σ_o is proportional to the local current density,[6,7,8] due to beam-impact ionization of the gas. Mathematically, the last assumption can be written $d\sigma_o/d\zeta = \kappa J_{bo}$, where ζ is the axial distance measured from the beam head toward the beam tail and κ is assumed to be constant. An important consequence[6,8] of this assumption is that $(\ell n\ \zeta)$, rather than ζ, is an ignorable coordinate for the governing equations of the equilibrium quantities. In addition, (f) perturbations of the electrical conductivity due to the effects of hose-perturbed beam currents are included self-consistently, as described in Ref. 8. Assumptions (a) - (f) have been adopted in the literature cited.

Instead of using the independent space-time variables (z,t) in the

laboratory frame, with z being the direction of beam propagation, we shall use (z,ζ) as independent variables in the description of the hose instability. Here, (z,ζ) is related to (z,t) through the transformation

$$\zeta = v_b t - z, \tag{1}$$

$$z = z, \tag{2}$$

and ζ may be regarded as the distance measured from the beam head toward the beam body, and is thus a "space-like" variable, while z becomes a "time-like" variable for a fixed distance ζ away from the beam head. In Eq. (1), v_b is the beam velocity and is very close to c, the speed of light. As mentioned in the last paragraph, $\ell n\ \zeta$ is an ignorable coordinate. Small amplitude perturbed quantities are then expected to vary as $\exp [- i\ \Omega_{ro} z - i\ \bar{\omega}\ \ell n\ \zeta]$ where Ω_{ro} is the "frequency" associated with "temporal" variation in z and $\bar{\omega}$ is the "wavenumber" associated with "spatial" variation in $\ell n\ \zeta$. The dispersion relation for the hose instability then relates the frequency Ω_{ro} to the wavenumber $\bar{\omega}$. Information concerning the absolute/convective behavior of the instability, as well as details of pulse propagation characteristics, may be extracted from such a dispersion relationship.[13]

It is convenient to use the normalized independent variables Z, ψ, defined by

$$Z = \Omega_{\beta o} z \tag{3}$$

$$\psi = (1/\lambda)\ \ell n\ (\zeta/a) \tag{4}$$

where a is the radius of the Bennett profile, $\Omega_{\beta o} \equiv (2|I_n|/I_A)^{1/2}/a$ is the betatron wavenumber, and $\lambda = \kappa I_b/2c$ is a dimensionless, positive constant. For propagation in air, a reasonable estimate[8] is $\lambda = 0.044\ I_b$ with I_b in kilo-amperes. Here, the net current I_n is the sum of the beam current I_b and the plasma current I_p, and $I_A \equiv (17\ \beta\ \gamma)$ kA is the Alfven-Lawson current. The normalized "frequency" $\Omega \equiv \Omega_{ro}/\Omega_{\beta o}$ and the normalized "wavenumber" $\lambda\bar{\omega}$ may then be introduced to the linearized quantities, all of which behave according to

$$\text{Linearized quantity} \sim e^{-i\,\Omega Z - i\lambda\bar{\omega}\psi}. \tag{5}$$

Under the assumptions stated at the beginning of this section, the spread mass model yields the dispersion relationship $D(\Omega,\bar{\omega}) = 0$, where

$$D(\Omega,\bar{\omega}) = [\omega - \bar{\omega}_1(\Omega)][\omega - \bar{\omega}_2(\Omega)] \tag{6}$$

and $\bar{\omega}_1$, $\bar{\omega}_2$ are defined as

$$\lambda\bar{\omega}_{1,2} = -\frac{i}{2}\,F\,(\Omega) \pm \frac{i}{2}\,[H(\Omega)]^{1/2}. \tag{7}$$

In Eq. (7),

$$F(\Omega) \equiv \lambda + \frac{f - G(\Omega)}{1 + f} \tag{8}$$

and

$$H(\Omega) \equiv F^2(\Omega) + 4\,\lambda G(\Omega), \tag{9}$$

where

$$G(\Omega) \equiv \int_0^1 d\eta \, \frac{6\eta(1-\eta)\Omega^2}{\eta - \Omega^2}$$

$$= 6\Omega^2 \left\{\left(\frac{1}{2} - \Omega^2\right) + \Omega^2(1-\Omega^2) \, \ell n \left(\frac{\Omega^2 - 1}{\Omega^2}\right)\right\} \qquad (10)$$

is the spread mass function introduced by Lee.[3] The derivation of the dispersion relationship (6) is given by Lampe, et al. in Ref. 8. Before we calculate the spatial amplification rate $\mathrm{Im}(\lambda\bar{\omega})$ as a function of the frequency Ω, we shall show[13] that the hose instability described by the dispersion relationship (6) is convective, regardless of the fraction of the return current f.

The following properties regarding the dispersion relationship will be needed: The functions $G(\Omega)$ and $F(\Omega)$, are analytic for all Ω with $\mathrm{Im}\Omega > 0$. The branch points of $G(\Omega)$ and $F(\Omega)$ are located at $\Omega = 0$, $\Omega = \pm 1$. Branch cuts originating from these branch points are introduced to render these functions analytic in the upper half Ω plane. Futhermore, $|G(\Omega)|$ and $|F(\Omega)|$ are bounded as $|\Omega| \to \infty$.

To show that the resistive hose instability as described by Eq. (6) is a convective instability, we need only to consider the response function

$$R(Z,\psi) = \int_L d\Omega \, S(\Omega) \, e^{-i\Omega Z} \int_{-\infty}^{\infty} d\bar{\omega} \, \frac{e^{-i\lambda\bar{\omega}\psi}}{D(\Omega,\bar{\omega})}, \qquad (11)$$

where $S(\Omega)$ denotes the spectrum of a source of excitation and L is the Bromwich contour on which $\mathrm{Im}(\Omega)$ is sufficiently large and positive. Absence of absolute instability is established if it can be shown that $R(Z, \psi) \to 0$ as "time" $Z \to \infty$, at any fixed value of "position" ψ, for any well-behaved

function $S(\Omega)$.[13]

The $\bar{\omega}$ - integral in (11), designated as $M(\Omega)$, can be carried out explicitly by the method of residues:

$$M(\Omega) = \int_{-\infty}^{\infty} \frac{d\bar{\omega}\, e^{-i\lambda\bar{\omega}\psi}}{[\bar{\omega} - \bar{\omega}_1(\Omega)][\bar{\omega} - \bar{\omega}_2(\Omega)]} . \tag{12}$$

It can easily be verified that as $\mathrm{Im}\Omega \to \infty$, $\bar{\omega}_1 \to -i$ and $\bar{\omega}_2 \to -i\lambda$. Thus, (12) yields

$$M(\Omega) = \begin{cases} 0 & , \text{for } \psi < 0 \\ 4\pi i \exp\left[-\frac{\psi}{2} F(\Omega)\right] \dfrac{\sinh\left[\frac{\psi}{2} H^{1/2}(\Omega)\right]}{H^{1/2}(\Omega)} & , \text{for } \psi > 0. \end{cases} \tag{13}$$

Equation (13) is valid for all Ω with $\mathrm{Im}\Omega \to \infty$. However, $M(\Omega)$ as given by (13) may be analytically continued for all Ω with $\mathrm{Im}\Omega > 0$ by observing that $M(\Omega)$ is singular only at the branch points of $F(\Omega)$, viz, $\Omega = 0, \pm 1$, and at the roots Ω_s of H. The singularities at Ω_s are removable singularities. Thus, $M(\Omega)$ is analytic for all $\mathrm{Im}\Omega > 0$, except at the branch points $\Omega = 0, \pm 1$. The inverse Laplace transform integral (11) may then be evaluated along the real Ω axis:

$$R(Z,\psi) = \int_{-\infty}^{\infty} d\Omega S(\Omega) e^{-i\Omega Z} M(\Omega). \tag{14}$$

Now, for any <u>fixed</u> value of ψ, $|M(\Omega)|$ is bounded for all real values of Ω. Thus, if the source function $S(\Omega)$ satisfies certain mild restrictions, (14)

yields $R(Z,\psi) \to 0$ as $Z \to \infty$ by the Riemann-Lebesgue Lemma. Note that this result is independent of f, the fraction of the plasma return current. We have thus proven that the hose instability is always convective.

We close this section with the following remarks. (a) The disturbance always propagates from the beam head toward the beam tail. This obvious fact is clearly indicated by Eq.(13), which shows that no perturbation on the beam can move faster than the beam head in the laboratory frame. (b) Convective growth is present, for if we let $\psi = VZ$ in Eq. (13b) for some fixed velocity V, $M(\Omega)$ may become exponentially large as $Z \to \infty$. We shall examine this point in more detail in the next section. (c) The detailed study of the evolution of the response function R as given by Eq. (14) is quite involved. We shall instead examine in the next section the evolution based on an approximation to the dispersion relation (6).

III. Propagation of Wavepackets

With the demonstration that the hose instability is convective, it is meaningful to consider the spatial amplification rate $\mathrm{Im}(\bar{\omega}\lambda)$ as a function of the frequency Ω. Shown in Fig. 1 is the growth rate $\mathrm{Im}(\bar{\omega}\lambda)$ as a function of real Ω obtained from the dispersion relationship (6) for the spread mass model. It is seen that the presence of a return current ($f < 0$) is destabilizing.[4,5] The return current yields a nonzero amplification rate at $\Omega = 0$ when $-f$ is sufficiently large. In fact, one can easily show from (6) that amplifying waves are possible for $\Omega = 0$ if $-f > \lambda/(1 + \lambda)$. Physically, the return current has a tendency to repel the beam axis from the magnetic field axis and thus weakens the restoring force.[4,5] Note from Fig. 1 that the unstable amplification band is restricted to $|\Omega| \lesssim 0.8$. The imaginary part of $(\bar{\omega}\lambda)$ is an even function of Ω and the real part of $(\bar{\omega}\lambda)$ is an odd function of Ω, Ω being real.

The dispersion relationship (7) is a complicated function of Ω which defies analytic study of the space-time evolution of a wave packet. To render the problem analytically tractable we shall approximate $\mathrm{Im}(\bar{\omega}\lambda)$ as a cubic polynomial in Ω and $\mathrm{Re}(\bar{\omega}\lambda)$ as a quadratic polynomial:

$$\mathrm{Im}(\bar{\omega}_a\lambda) = a_o + a_2\Omega^2 - a_3\Omega^3, \quad (\Omega > 0) \tag{15}$$

$$\mathrm{Re}(\bar{\omega}_a\lambda) = - b_2\Omega^2, \tag{16}$$

where a_o, a_2, a_3, b_2 are nonnegative constants. Curves of $\mathrm{Im}(\bar{\omega}_a\lambda)$ for various combinations of these constants are shown in Fig. 2. Comparing Fig. 1 with Fig. 2, it is seen that the amplification rate $\mathrm{Im}(\bar{\omega}\lambda)$ from Eq. (7) can be approximated quite well by $\mathrm{Im}(\bar{\omega}\lambda)$ of Eq. (15). However, Eq. (16) is a poorer

approximation to $\mathrm{Re}(\bar{\omega}\lambda)$. Equations (7)-(10) show that $\mathrm{Re}(\bar{\omega}\lambda)$ reduces to a sixth-degree polynomial in Ω, for large Ω. If the beam profile were Gaussian rather than Bennett, the spread mass model would lead to a fourth degree polynomial.

To correct this deficiency, we shall bracket the real shape of $\mathrm{Re}(\bar{\omega}\lambda)$ by allowing b_2 to range from zero to infinity. In this way, we can determine whether wave group convection is sensitive to the model chosen. We also note from Figs. 1 and 2 that the constant a_o in (15) may be used to represent the amount of the return current, which leads to a nonvanishing value of $\mathrm{Im}(\bar{\omega}\lambda)$ at $\Omega = 0$.

If the spectrum $S(\Omega)$ of the source is an even function of Ω, the integral in (14) may be carried over the range $0 \leq \Omega \leq \infty$ since $\mathrm{Im}(\bar{\omega}\lambda)$ is an even function and $\mathrm{Re}(\bar{\omega}\lambda)$ is an odd function of Ω. Thus, instead of carrying out the complicated integral (14), we are led to consider the simplified integral

$$R_a(Z,\psi) = \int_o^\infty d\Omega S(\Omega) e^{-i\Omega Z - i\lambda\bar{\omega}_a(\Omega)\psi} \tag{17}$$

where $\bar{\omega}_a(\Omega)$ is the approximated propagation constant [cf. (15) and (16)]. If we further restrict consideration to the case $S(\Omega) = 1$, substitution of (15) and (16) into (17) yields

$$R_a(Z,\psi) = e^{a_o\psi}\, I(Z,\psi) \tag{18}$$

where

$$I(Z,\psi) = \int_o^\infty d\Omega \exp\left\{-i\Omega Z + \psi\left[(a_2 + i\, b_2)\,\Omega^2 - a_3\Omega^3\right]\right\} \tag{19}$$

is somewhat similar to an integral representation of the Airy function. Note that the effect of the return current (a_o) is factored out in (18) and the remaining integral I defined in (19) is independent of a_o. It is readily demonstrated from (19) that $I(Z,\psi) \to 0$ as $Z \to \infty$ at any fixed positive value of ψ. Thus, the approximate response function $R_a(Z,\psi)$ is consistent with our earlier conclusion that absolute instability is absent, regardless of the return current.

The evolution of $I(Z,\psi)$ is best visualized by setting

$$\psi = VZ \tag{20}$$

with V fixed, but letting $Z \to \infty$. The result function I(Z,VZ) may then be interpreted as the evolution of disturbances recorded by an instrument which travels at a normalized velocity V moving from the beam head toward the beam tail. The integral I is then a function of V, a_2, b_2 and a_3, and the asymptotic response

$$|R_a(z,\psi)| \sim e^{p\psi} \tag{21}$$

may be regarded as the spatial dependence recorded by the moving instrument. Again $p = p(V)$ when the constants a_o, a_2, a_3, b_2 are fixed.

We have used the method of steepest descent to evaluate the asymptotic behavior ($Z \to \infty$) of I(Z,VZ) as defined in Eq. (19) for various combinations of a_o, a_2, a_3, b_2 and V. The procedure is rather involved and is outlined in the Appendix. Our findings are summarized below.

Since there are five free parameters, it is convenient to introduce a complex constant

$$\Omega_1 \equiv (a_2 + i\, b_2)/3a_3 \equiv |\Omega_1| e^{i\alpha} \tag{22}$$

where $\alpha \equiv \tan^{-1}(b_2/a_2)$ ranges from zero to $\pi/2$ as b_2 varies from zero to infinity.

The value of α can be specified by requiring that the value of $\mathrm{Re}(\bar{\omega}\lambda)$ or its derivative at Ω_M, the frequency at which maximum amplification is expected, match the correct value from Eqs. (7)-(10). The value of α typically lies in the range between 15^o and 60^o. Over this range, we shall see that the most important features of the results are not sensitive to α; this justifies the use of our representation (16).

Instead of using V, we find it convenient to represent the data in terms of U, where

$$U \equiv 3a_3 |\Omega_1|^2 V. \tag{23}$$

We normalize the spatial amplification rate p with respect to p_M, the maximum value of amplification rate expected from the approximation dispersion relation (15),

$$p_M \equiv \mathrm{Max}[\mathrm{Im}(\bar{\omega}_a \lambda)] = a_o + \frac{4}{27}\frac{a_2^3}{a_3^2}. \tag{24}$$

Note also that p_M occurs at $\Omega = \Omega_M$, where $\Omega_M = 2a_2/3a_3$, at which the "group velocity" V_M is given by

$$V_M = \left|\frac{\partial(\lambda\bar{\omega}_a)}{\partial\Omega}\right|^{-1}_{\Omega=\Omega_M} = \frac{3a_3}{4a_2 b_2}. \tag{25}$$

By examining the asymptotic response I(Z,VZ) as $Z \to \infty$, in a manner

described in the Appendix, the normalized spatial amplification rate p/p_M as a function of U for various values of $\alpha(b_2)$ is shown in Fig. 3, where we set $f = a_o = 0$. It is noted from this figure that the maximum value of p is indeed p_M. This result may be proved in a rigorous manner. Note also from this figure that there is a minimum velocity U_{min} for amplification to occur, which is typically about 1/3-1/2 of the velocity U_M for peak amplification. In other words, an observer moving backward in the beam at a normalized velocity U which is less than U_{min} always sees the disturbance decaying away at late times. It would not be obvious from a casual examination of the dispersion relation that U_{min} is considerably less than U_m. Note also that p remains nonnegative as $U \to \infty$. This is due to our use of Lee's[3] reduced form of Maxwell's equations (appropriate to highly relativistic paraxial beams) to derive Eq. (7). In Lee's form, the field equations are diffusive when the plasma is resistive; signal propagation can occur at infinite speed for diffusion equations. If the exact Maxwell equations were used, there would of course be no signal propagation at $V > c$. This deficiency in Lee's formulation is of little practical significance. Shown in Figs. 4 and 5 are the values of p/p_M for the two cases $f = -0.4$ and -0.6 [cf. Fig. 2.] Again, the minimum speed U_{min} of propagation for the amplifying waves is about 1/2 to 1/3 of that associated with maximum amplification, for the range of parameters surveyed. This mimimum velocity is compared with $U_M = 3a_3|\Omega_1|^2 V_M$ in Fig. 6, where V_M is defined in Eq. (25). Of course, U_{min}/U_M is model-dependent, but $U_{min} \lesssim \frac{1}{2} U_M$ over the range of parameters surveyed. In fact, for low values of $\alpha(b_2)$, U_{min} is substantially less than U_M (Fig. 6).

In all cases, the value of U_{min} is not particularly sensitive to the value assumed for b_2, i.e. for α. Thus, it would appear that our approximation (16) is adequate, even though there is no well-defined way to specify b_2.

IV. Remarks

In this paper, we have performed a quantitative study of the evolution of the convective hose instability based on simplified models applicable to the main body of the beam. We find that the instability is always convective in the beam frame, regardless of the return current. At late time, the peak of the disturbance convects backward in the beam at a dimensionless velocity $U_M = \left|\frac{\partial(\lambda\bar{\omega})}{\partial\Omega}\right|_{\Omega = \Omega_M}$, while amplifying at a rate $P_M = \mathrm{Im}[\lambda\bar{\omega}(\Omega_M)]$, where Ω_M is the most unstable value of Ω, i.e. the value for which $\mathrm{Im}\bar{\omega}(\Omega_m)$ is largest. However the disturbance also spreads out as it convects backward, so that the trailing edge of the growing disturbance moves at a considerably slower velocity U_{min}, which we have shown to be somewhere between 1/3 U_M and 1/2 U_M. Along characteristics moving backward in the beam at velocities less than U_{min}, the disturbance damps away. More precise specification of U_{min} is not possible, within the limitations of the simple model used. The mutual influence of beam head erosion[11,12] and the convection of hose wavepackets remained to be assessed. As a function of ζ [rather than of $\psi \equiv \lambda^{-1}\, \ell n(\zeta/r_o)$], the instability grows fastest and convects slowest just behind the pinch point, near the front of the beam. It is possible that erosion can significantly enhance instability growth when the erosion speed is comparable to the convection speed in this region, thus causing the region of the beam that is most hose-unstable to move backward in ζ along with the hose wave packet.

Acknowledgments

We wish to thank Drs. Richard Hubbard and Glenn Joyce for helpful discussions, particularly in regard to multicomponent simulations and linearized particle simulations that support some of the ideas developed here. We are also grateful to Dr. Bertram Hui for helpful discussions. This work was supported by the Defense Advanced Research Projects Agency under ARPA Order 4395, Amendment No. 9. This work was performed while one of us (Y.Y. Lau) was with Science Applications, Inc.

Appendix

Asymptotic Evolution of $I(Z,\psi)$

In this appendix, we outline the procedure used to evaluate the integral $I(Z,\psi)$ given by Eq. (19) of the main text, with the understanding that $\psi = VZ$, where V is a pre-assigned positive constant and $Z \to \infty$. The saddle point method will be used. Note that there are two saddle points for the exponents in the integral of (19). Thus, the asymptotic expression to (19) in general contains three terms: the end point contribution arising in the neighborhood of $\Omega = 0$, and the saddle point contributions near the two saddle points. An inspection of (19) shows that the end point contribution is less significant than the saddle point contribution, and its role will thus be ignored. The location of the saddle points determines which saddle point contribution will dominate the integral (19), as we shall show here.

With the transformation

$$\Omega' \equiv (a_3\psi)^{1/3} (\Omega - \Omega_1), \tag{A-1}$$

where Ω_1 is defined by Eq. (22) of the main text, it can be shown that $I(Z,\psi)$ may be written as

$$I(Z,\psi) = \text{Const} \times \psi^{-1/3} e^{E_1(Z,\psi)} J(Z,\psi) \tag{A-2}$$

where

$$E_1(Z,\psi) = \Omega_1(3a_3\psi\ \Omega_1^2 - iZ) - a_3\psi\ \Omega_1^3$$

and

$$J(Z,\psi) \equiv \int_{\Omega_1'}^{\infty} d\Omega' \, e^{-\Omega'^3 + 3\,\Omega_s'^{-2}\,\Omega'} . \qquad \text{(A-3)}$$

In this equation,

$$\Omega_1' \equiv -(a_3\psi)^{1/3}\,\Omega_1 \qquad \text{(A-4)}$$

$$\Omega_s'^{-2} \equiv \Omega_1'^{-2} - \frac{iZ}{3(a_3\psi)^{1/3}} \qquad \text{(A-5)}$$

and the upper limit of the path integral in (A-3) approaches the positive $\mathrm{Re}(\Omega')$ axis (Fig. 7). From (A-3), we then see that the saddle point contribution to I depends just on the complex quantities Ω_1' and Ω_s'. These latter quantities, of course, depend on a_2, b_2, a_3, Z, ψ, by Eqs. (A-4) and (A-5).

The saddle points for $J(Z, \psi)$ are located at $\Omega' = \Omega_{s1}'$ and $\Omega' = \Omega_{s2}'$ in the complex Ω' plane, where

$$\Omega_{s1}'^{-2} = \Omega_{s2}'^{-2} = \Omega_s'^{-2}, \qquad \text{(A-6)}$$

which is defined in (A-5). If either Ω_{s1}' or Ω_{s2}' lie in any one of the shaded regions of Fig. 7, the contribution due to that saddle point will be dominant (over that due to the other saddle point) provided the contour for (A-3) may be detoured along steepest descent curves which pass through that saddle point.

As an example, consider the values of a_2, b_2, a_3, Z, ψ such that the saddle points Ω_{s1}' and Ω_{s2}' are depicted as in Fig. 8 (left). The contribution to J due to Ω_{s1}' will be subdominant whereas that due to Ω_{s2}' will be dominant. The steepest descent curves which pass through

Ω_{s1}' and Ω_{s2}' are also sketched in Fig. 8 (left). The initial point Ω_1' of integration always lies in the third quadrant of the Ω' plane, and the path of integration originating from Ω_1' is also depicted in Fig. 8 (left). Now, consider domains A, B, C, D, all of which lie in the third quadrant and are bounded by the steepest descent curves passing through Ω_{s2}'. [Fig. 8 right]. If the initial point of integration Ω_1' lies in A or B, only the contribution around Ω_{s1}' will be picked out by detouring the path of integration as shown in Fig. 8b. On the other hand, if Ω_1' lies within domains C, D, the path of integration is detoured so that both saddle points Ω_{s1}' and Ω_{s2}' are passed through. Of course, in the latter case, the contribution due to Ω_{s2}' would dominate. It is to be noted that the topology of the steepest descent curves change as Ω_{s1}' and Ω_{s2}' vary. Based on a systematic examination of the relative position between Ω_1' and Ω_{s1}', we are able to determine the relevant saddle point contributions to J. In this way, the data shown in Fig. 3-5 of the main text is generated.

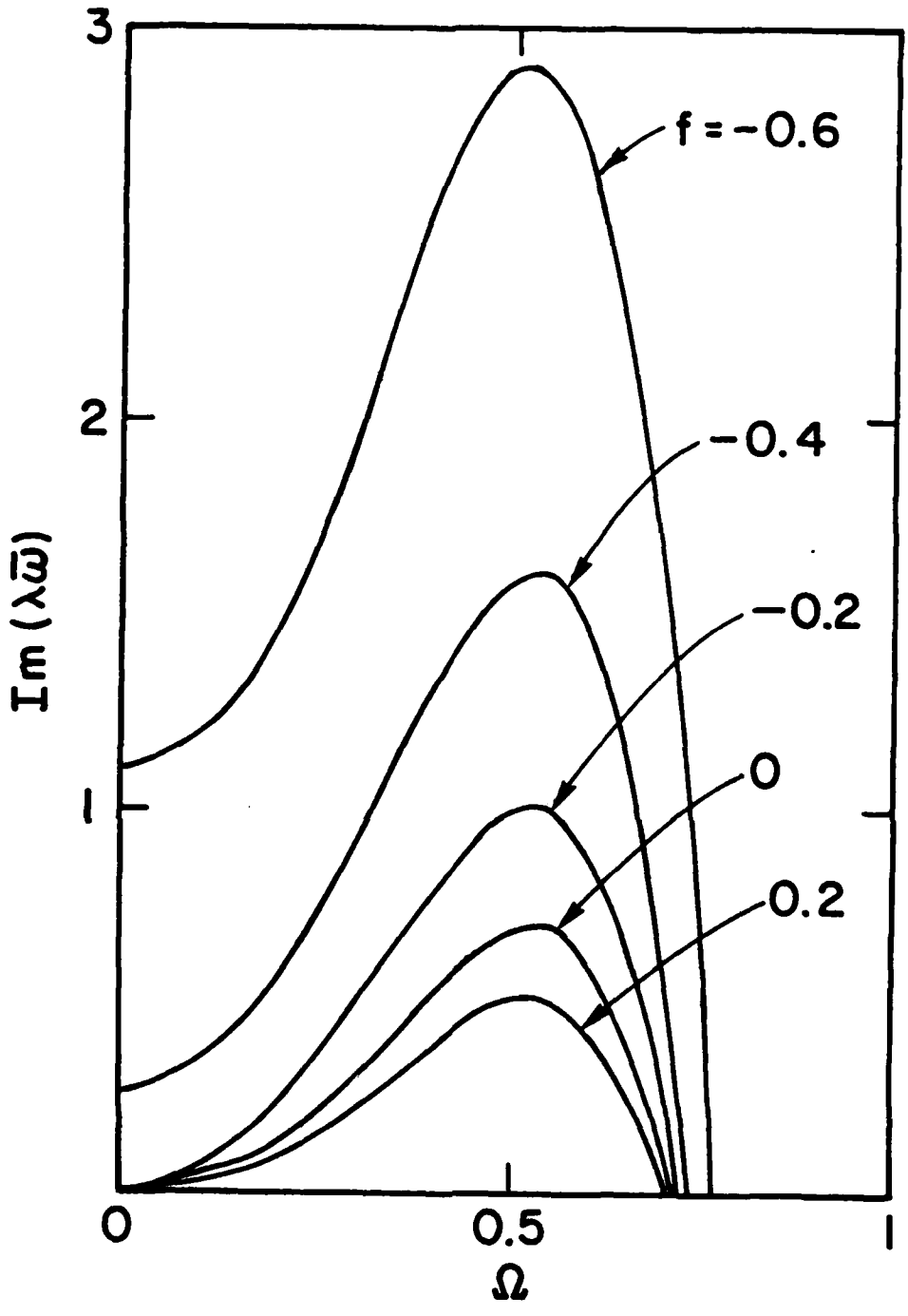

Figure 1

The normalized spatial amplification rate $\mathrm{Im}(\lambda\bar{\omega})$ as a function of normalized frequency Ω for several values of the return current fraction f, as given by the spread mass model including a self-consistent conductivity model, Eq. (7).

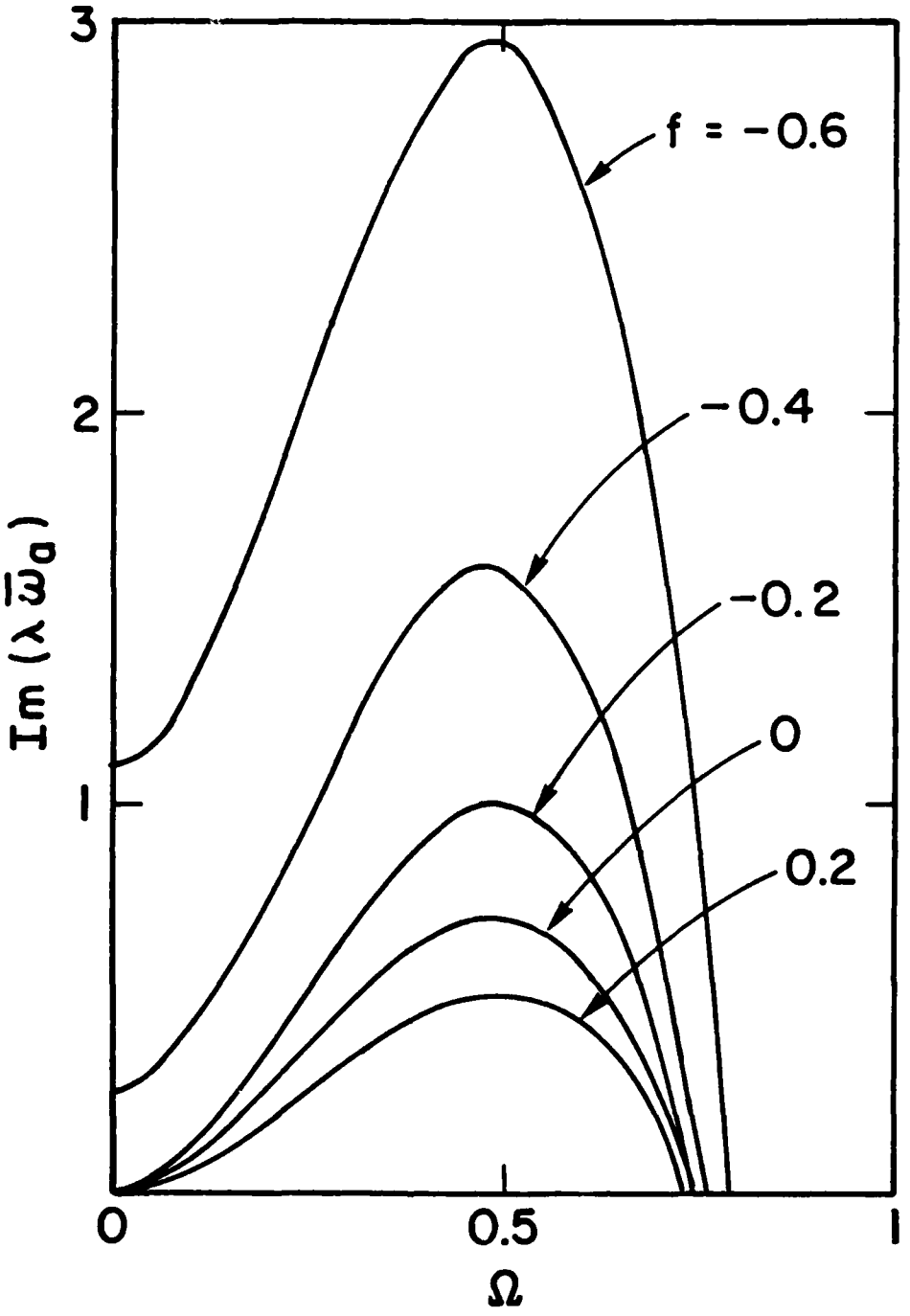

Figure 2

The approximate dispersion relation $\mathrm{Im}(\lambda\bar{\omega}_a) \equiv a_o + a_2\Omega^2 - a_3\Omega^3$, Eq. (15). To match the result of Eq. (7) for each of the various values of f, we have chosen the following values of a_o, a_2, a_3: f = − 0.6: (a_o, a_2, a_3) = (1.1, 21.84, 29.12); f = −0.4: (0.26, 16.08, 21.44); f = − 0.2: (0, 12, 16); f = 0: (0, 8.4, 11.2); f = 0.2: (0, 6.12, 8.16).

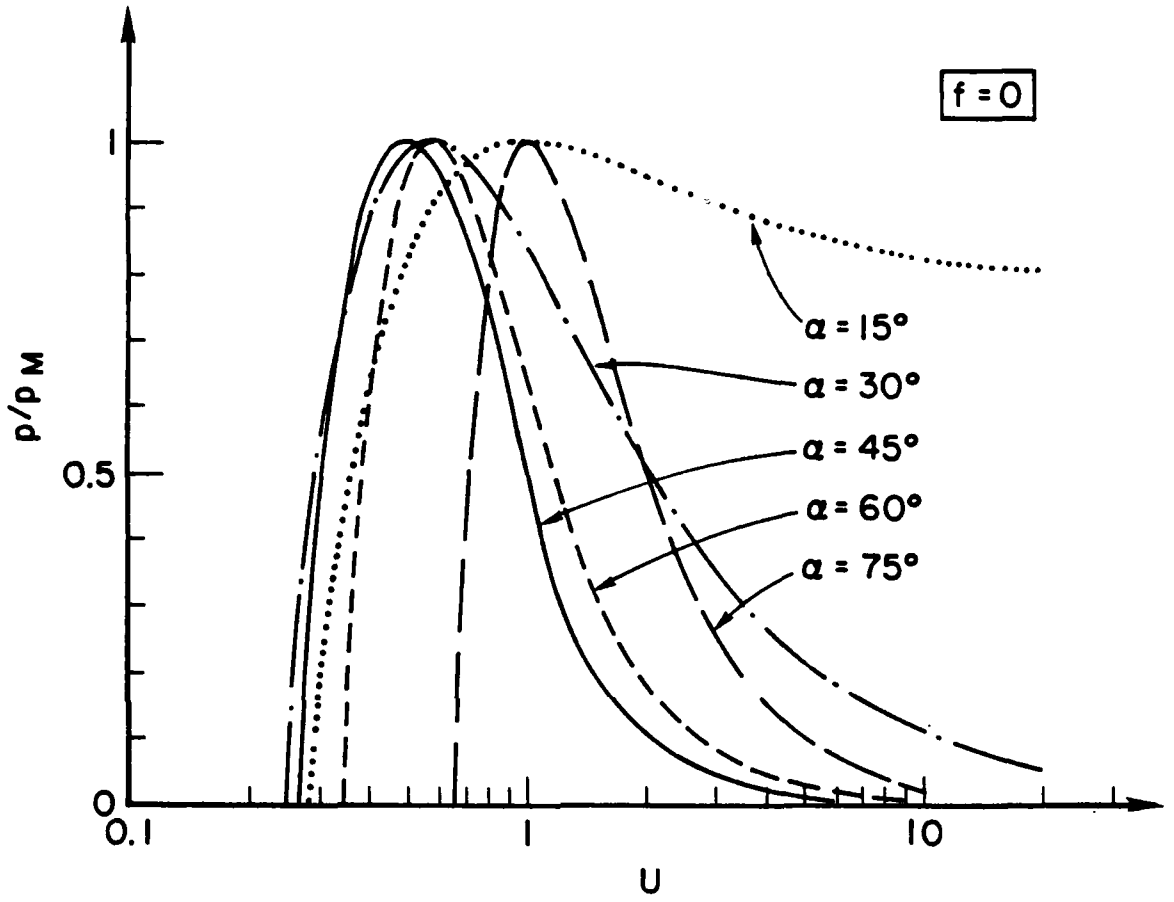

Figure 3

Value of the amplification rate p as recorded by an instrument moving backward in the beam at scaled velocity U, for a case with f = 0. The rate p is normalized to the peak amplification rate p_M. Each curve represents a different choice of the parameter $\alpha = \arctan(b_2/a_2)$.

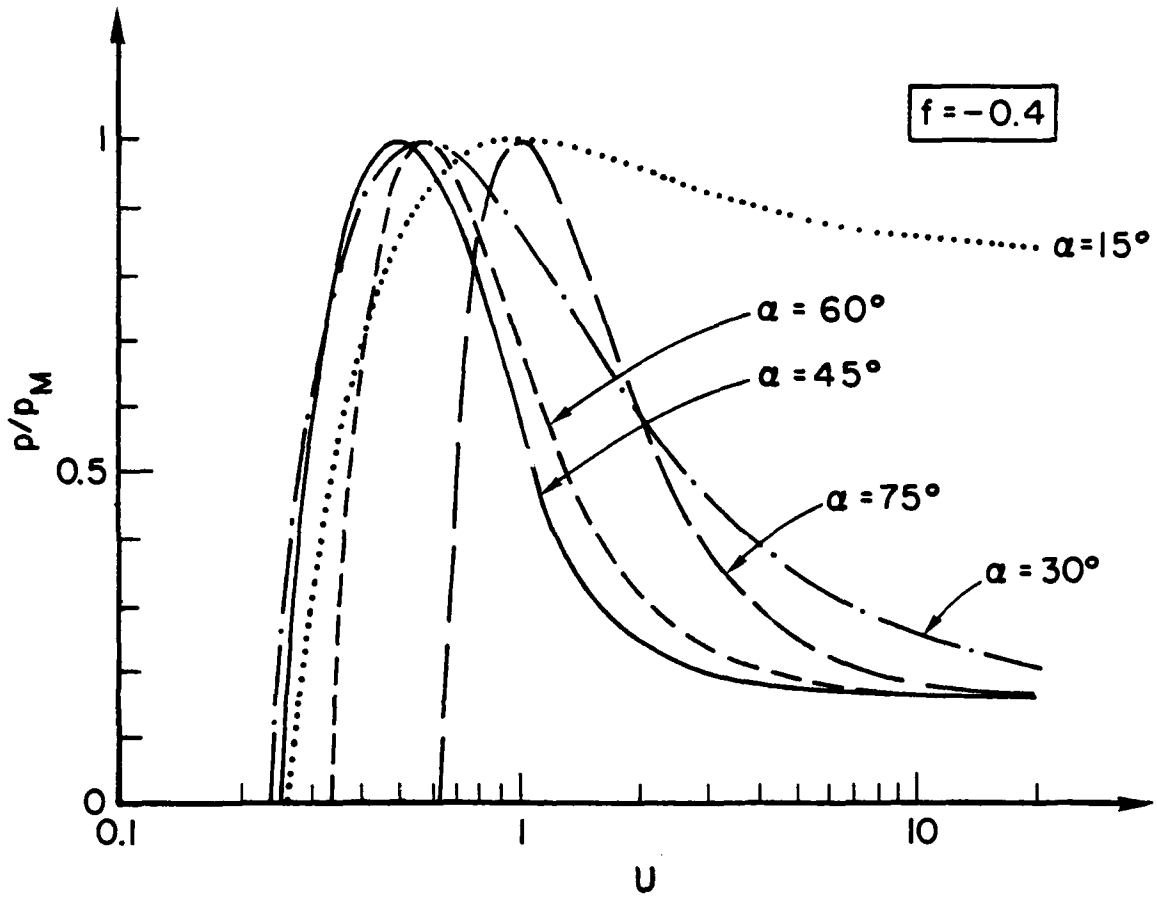

Figure 4

Same as Fig. 3, except that f = − 0.4.

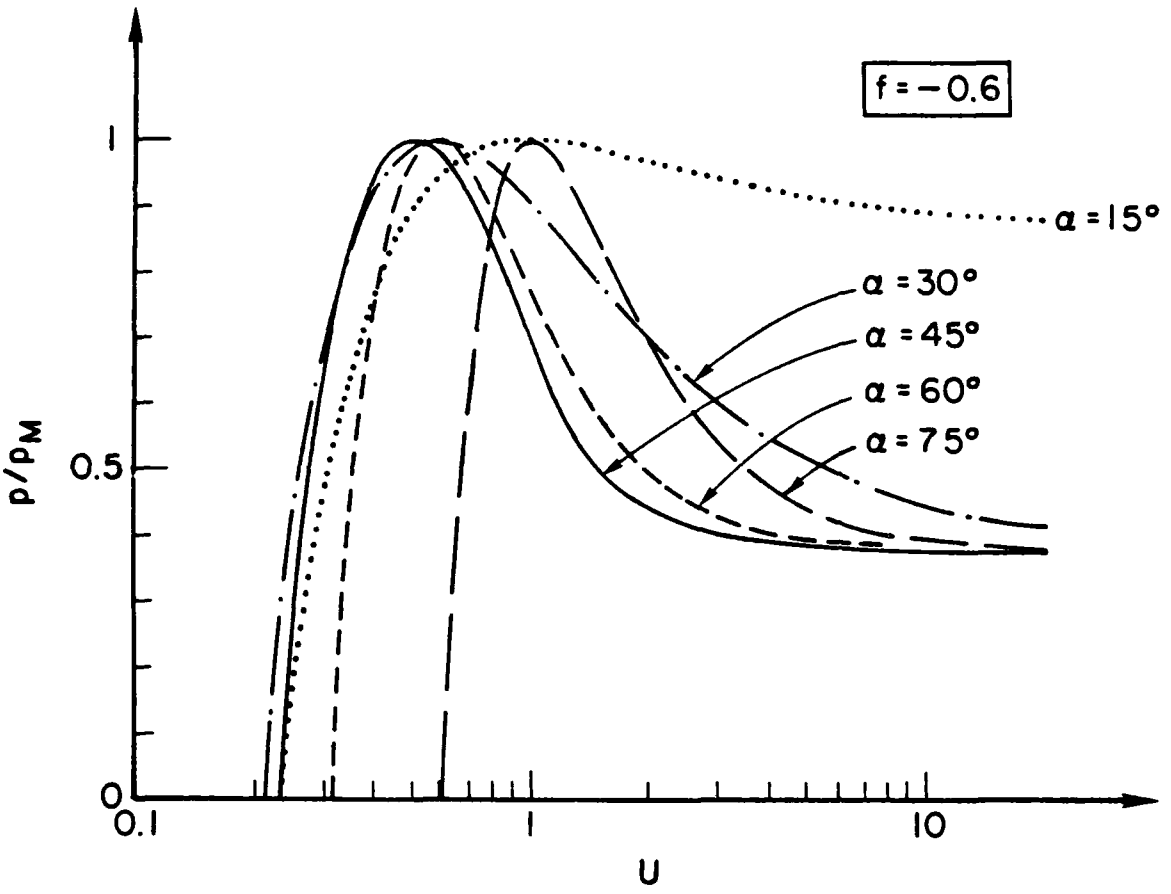

Figure 5

Same as Figs. 3 and 4, except that f = - 0.6.

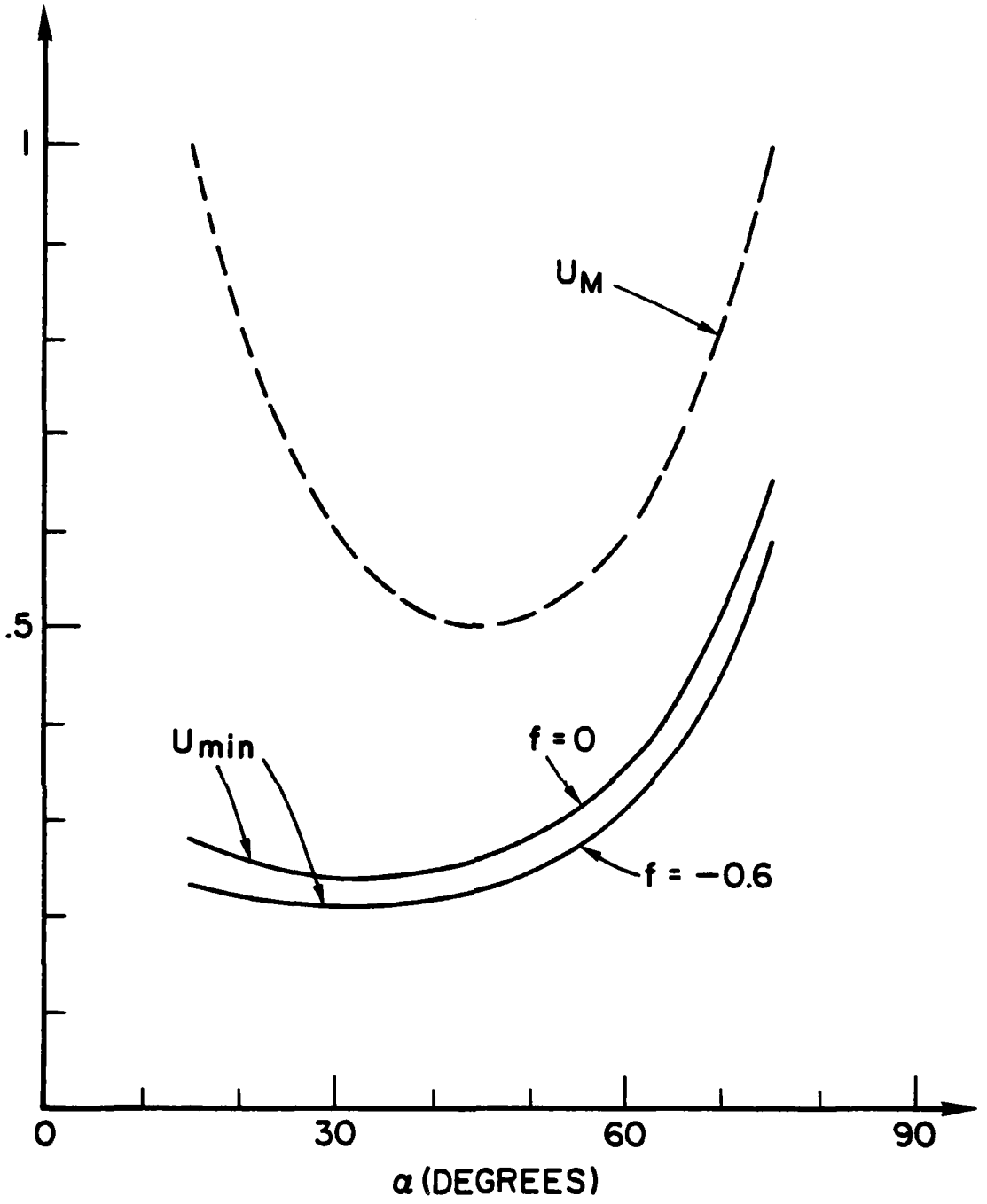

Figure 6

Values of the scaled velocity U_M that yields the maximum amplification rate, and of the mimimum scaled velocity U_{min} that yields any amplification, each as a function of the numerical parameter α. U_M (α) is independent of f, while U_{min} (α) depends weakly on f. The ratio U_{min}/U_M depends weakly on both f and α.

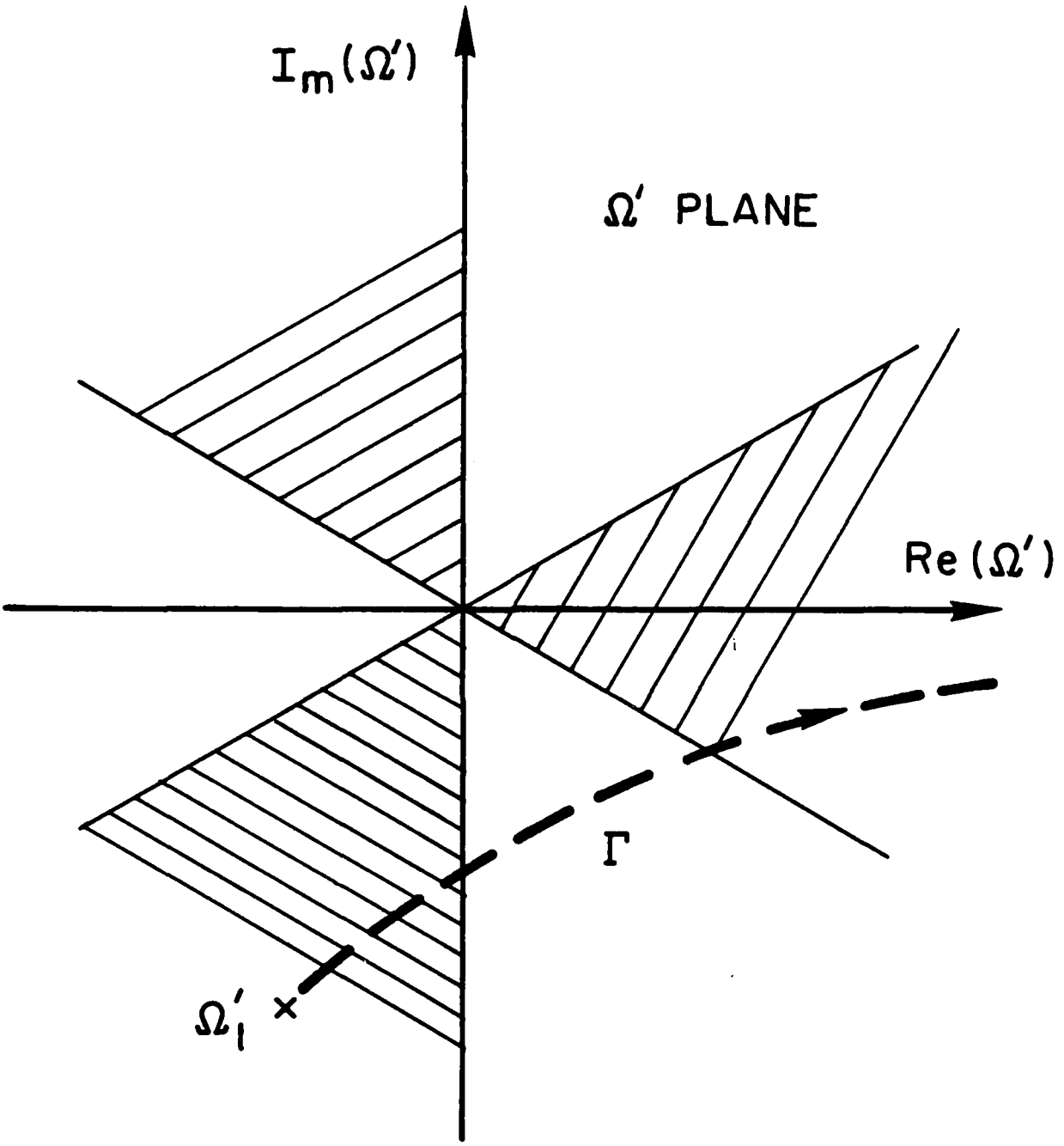

Figure 7

The path of integration Γ in the complex Ω' plane. The integrand in Eq. (A3) tends to zero as $|\Omega'| \to \infty$ in the shaded domains, which are sixty degree sectors.

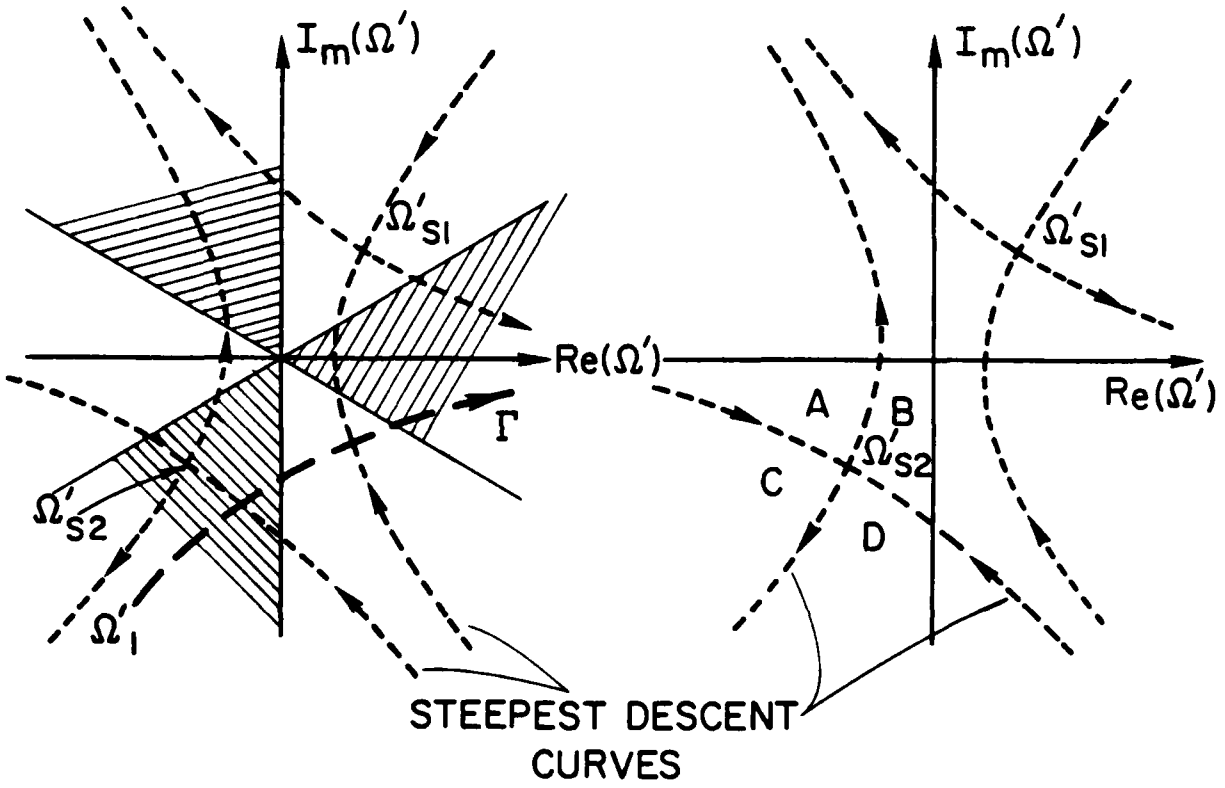

Figure 8

(a) Left. The contour Γ and the steepest descent curves which pass through saddle points Ω'_{s1} and Ω'_{s2}.

(b) Right. Domains A, B, C, D in the third quadrant of the Ω' plane in which Ω'_1 lies.

References

1. E. J. Lauer, R. J. Briggs, T. J. Fessenden, R. E. Hester, and E. P. Lee, Phys. Fluids 21, 1344 (1978).
2. D. S. Prono, et al., Preprint UCRL-88590, Lawrence Livermore Laboratory, Dec 7, 1982.
3. E. P. Lee, Phys. Fluids 21, 1327 (1978).
4. W. M. Sharp, M. Lampe and H. S. Uhm, Phys. Fluids 25, 1456 (1982).
5. H. S. Uhm and M. Lampe, Phys. Fluids 23, 1574 (1980).
6. M. Lampe, W. M. Sharp, G. Joyce, R. F. Hubbard, and H. S. Uhm, in the Proceedings of the Fourth International Conference on High Power Electron and Ion Beam Research and Technology, Ecole Polytechnique, Palaiseau, France, 1981, p. 145.
7. M. Lampe, G. Joyce and R. F. Hubbard, in Proceedings of the Fifth International Conference on High Power Particle Beams, San Francisco, 1983.
8. M. Lampe, W. M. Sharp, and R. Hubbard, NRL Memo Report 5140, 1983.
9. M. N. Rosenbluth, Phys. Fluids 3, 932 (1960).
10. S. Weinberg, J. Math. Phys. 5, 1371 (1964); 8, 614 (1967).
11. E. P. Lee, Lawrence Livermore National Laboratory Report UCID-18768 (1980).
12. W. M. Sharp and M. Lampe, Phys. Fluids 23, 2383 (1980).
13. R. J. Briggs, Electron Stream Interactions with Plasmas, Ch. 2, MIT Press (1964).